(3+) #4 Project 87-1-X921 +
Put in Notebook

Date 12 January 1979

INTEROFFICE
MEMORANDUM

Subject Mathematical Modelling of Solids Buildup in Tubular Dissolvers (87-1-X921)

To G. W. Roberts — Corporate R&D
(Location, Organization, or Department)

From R. F. Weimer — Corporate R&D
(Location, Organization, or Department)

cc: (w/o Attach.)

Also data in monthly Reports

E. N. Givens
R. W. Skinner
D. H. S. Ying

Attached is a copy of the paper which Dave Ying has identified as a likely basis for modelling his solids accumulation data. The model is based on diffusion superimposed on bulk flow - as you have suggested - and it has the following features:

1. The particle flow equation is numerically integrated over all the particle sizes in the system.

2. Liquid velocity is found to be important in determining the particle concentration profile (see Figure 4).

3. Stokes' law (or a more generalized drag coefficient) is used to predict particle/liquid slip velocities.

4. For co-current upflow of solids, liquid, and gas, a solution to the unsteady-state equation of particle flow is required; a rigorous analytical solution could not be found.

I think that a set of solutions to the transient particle accumulation equations - covering the required ranges of the variables - could be generated relatively easily by numerical techniques. These solutions could be compared to the results to see if the model fits. During Dave Ying's and my discussion of this program with Ken Smith on 10 January, Ken indicated that he did not recommend using calculations of the moments as a basis for fitting the mixing data.

The results of the solids accumulation tests with ethanol/water mixtures as the liquid phase may prove to be difficult to explain. (In these tests, the steady-state concentration in the column was independent of position, but was higher than the feed or outlet concentration.) Ken suggested that surface-active effects, with particles being carried completely up the column at

liquid/gas interface of the bubbles, might provide an explanation, provided that some of the particles settle back into the column when the bubbles reach the top. An alternative hypothesis is that liquid mixing is very different in this system due to the higher viscosity and/or the presence of the large number of small bubbles.

Bob

R. F. Weimer

aee

Attach.

CATALYST SUSPENSION IN GAS-AGITATED TUBULAR REACTORS

D. R. COVA

Research Department, Organic Chemicals Division, Monsanto Co., Saint Louis, Mo.

The suspension of catalyst in a gas-agitated 1.8-inch i.d. reactor was observed for the cases of Raney nickel catalyst in water and in acetone. The effects of gas and liquid flow rates were investigated. A model was developed which predicts the catalyst profile in a reactor as a function of physical properties and operating conditions, and was applied with success to both laboratory and plant scale reactors.

The application of reaction kinetics to the scale-up and design of tubular reactors necessitates a knowledge of the catalyst concentration within the reaction zone. In the case of heterogeneous catalysts such as Raney nickel this is a complicating factor, in that the catalyst particles have a fall velocity with respect to the liquid in which they are suspended. Because of this, the catalyst concentration in the reactor will be a function not only of catalyst concentration in the feed stream, but also of the direction and magnitude of the liquid velocity through the reactor, mixing characteristics of the system, position in the reactor, and physical properties of the liquid and the catalyst.

Theory

The motions of particles suspended in a liquid medium in a gas-sparged tubular reactor may be analyzed through consideration of the various components of flow. Thus, particles in a still liquid will exhibit a downward flow under the influence of gravity. This fall velocity of the particles, V_p, is a function of the particle size and shape, particle and liquid densities, and liquid viscosity. If the liquid medium is flowing in a vertical direction, its velocity, V_L, will be superimposed on the particle fall velocity. In downward liquid flow the velocity of the particles, V_p, with respect to laboratory coordinates will be $V_p = V_L + V_p$. In the countercurrent tubular reactor then (gas flowing up and liquid flowing down) the particle concentration in the reactor will be less than, or at most equal to, the concentration in the feed stream, since the particles in the reactor have a greater bulk velocity than the liquid. In the case of upward liquid flow, $V_p = V_L - V_p$. Thus, in the concurrent tubular reactor (gas and liquid both flowing upward) the concentration of particles in the reactor will be greater than, or at least equal to, the feed concentration.

In gas-agitated reactors there is a third motion to be considered, that of mixing. The flow of gas through a liquid in a tube has been shown to induce considerable mixing of the liquid (*1, 6*). This flow of the liquid will bring about a similar flow of the solid particles. In the cases of both liquid and solids this flow has been successfully represented by a diffusion mechanism (*1, 3, 4, 6*). Particle motion in a tubular reactor may then be described as diffusion superimposed on a bulk flow.

In the following this description of particle motion is placed on a quantitative basis.

Raney nickel and similar catalysts are composed of particles ranging over a wide spectrum of sizes. For ease of analysis, the mathematical treatment which follows is concerned with only one species—i.e., size—of particle. When necessary, the analysis is expanded to cover all the species involved.

For a differential element of reactor volume the continuity equation for a given species of catalyst particles may be written as:

$$\frac{\partial C}{\partial t} + \nabla \cdot (\bar{n}_p) = 0 \qquad (1)$$

With the assumption that there are no radial gradients, Equation 1 reduces to:

$$\frac{\partial C}{\partial t} + \frac{\partial}{\partial x}(n_p) = 0 \qquad (2)$$

The mass flux, n_p, may be represented by a modification of Fick's law. The modification is necessary in order to take into account the effect of gravitational forces on the catalyst particles. The resultant equation is:

$$n_p = \frac{C(n_p + n_l)}{\rho} + CV_p - \epsilon \frac{\partial C}{\partial x} \qquad (3)$$

where CV_p represents the effect of gravitational force on the particles (V_p being the terminal fall velocity of the particles).

It is now assumed that n_p is small relative to n_l, so that

$$\frac{n_p + n_l}{\rho} = V_L \qquad (4)$$

Substituting into Equation 2 with the above assumptions, there is obtained:

$$\frac{\partial C}{\partial t} + (V_L + V_p)\frac{\partial C}{\partial x} - \epsilon \frac{\partial^2 C}{\partial x^2} = 0 \qquad (5)$$

In arriving at Equation 5 it has been assumed (in the application of Fick's law) that particle mixing can be described here by a diffusion mechanism. This assumption and the one regarding radial gradients are not universally applicable in these gas-sparged systems. The conditions under which these assumptions break down are discussed by Aego and Cova (*1*). For the cases taken under consideration here these assumptions present no difficulty.

There are two cases to be considered, concurrent and countercurrent operation. In countercurrent operation, the liquid feed containing catalyst particles enters at the top of the reactor, while gas is fed in at the bottom. Since the particles have some definite fall velocity, they tend to pass down through

catalyst concentration in the tube is less than it is in the feed. Because of this, steady state is achieved in a relatively short time. Thus, only the steady state is of importance here, and Equation 5 is modified to:

$$0 = v = -(V_L + V_P) \times \frac{\partial C}{\partial x} + \epsilon \frac{\partial^2 C}{\partial x^2} \qquad (6)$$

The general solution of Equation 6 is:

$$C = A + B \exp(V_L + V_P)\frac{x}{\epsilon} \qquad (7)$$

Two boundary conditions are now required.

At the top of the reactor ($x = L$),

$$V_L C_F = (V_L + V_P)C_L - \epsilon \left.\frac{\partial C}{\partial x}\right|_L \qquad (8)$$

At the bottom of the reactor ($x = 0$),

$$V_L C_F = (V_L + V_P)C_F - \epsilon \left.\frac{\partial C}{\partial x}\right|_0 \qquad (9)$$

The first boundary condition, Equation 8, expresses the fact that the rate of feed into the reactor must equal the flow from the inlet plane by bulk flow and diffusion. The meaning of Equation 9 is completely similar.

Application of these boundary conditions to Equation 7 yields the following:

$$C = C_F \left\{ \frac{|V_L|}{|V_L| + |V_P|} + \left(1 - \frac{|V_L|}{|V_L| + |V_P|}\right) \exp\left[-(|V_L| + |V_P|)\frac{x}{\epsilon} \right] \right\} \qquad (10)$$

Equation 10 defines the particle concentration at any level, x, in the tube as a function of the liquid and particle fall velocities and the eddy diffusivity. For the case of a totally mixed reactor ($\epsilon \to \infty$), Equation 10 reduces to $C = C_F$ for all values of x. For the case of plug flow ($\epsilon \to 0$), Equation 10 reduces to $C = C_F \times |V_L|/(|V_L| + |V_P|)$ for all x. For the case of partial mixing ($0 < \epsilon < \infty$), the concentration lies between $C_F \times |V_L|/(|V_L| + |V_P|)$ and C_F, increasing to C_F as $x \to 0$. According to Equation 10, an increase in mixing, an increase in liquid velocity, and a decrease in fall velocity all lead to higher and more uniformly distributed catalyst concentrations.

Equation 10 is applicable only to particles of a given species. To apply the equation to a catalyst such as Raney nickel, it is necessary to integrate the equation over all the particle sizes present in the catalyst. This can be done by a numerical integration using the log-normal distribution function to define the particle size–concentration relationship. Stokes' law provides the relation between particle diameter and fall velocity.

The case for concurrent flow is more complex. Here, all the feeds enter at the bottom of the tube. All catalyst particles tend to concentrate in the tube. In fact, particles for which $|V_P| > |V_L|$ leave the reactor only because of the flows caused by mixing. In the case of Raney nickel catalyst, it was found under the conditions of the laboratory experiments that an extremely long time would have been required to build up significant concentrations of these heavy particles and achieve the steady state. For concurrent operation then, the transient state cannot be ignored.

For the steady-state solution the following boundary conditions are sufficient:

$$V_L C_F = (V_L - V_P)\left.C\right|_0 - \epsilon \left.\frac{\partial C}{\partial x}\right|_0 \qquad (11)$$

At $x = L$ (top and exit end),

$$V_L C_F = (V_L - V_P)C_F - \epsilon \left.\frac{\partial C}{\partial x}\right|_L \qquad (12)$$

The steady-state solution then is:

$$C = C_F \left\{ \frac{|V_L|}{|V_L| - |V_P|} + \left(1 - \frac{|V_L|}{|V_L| - |V_P|}\right) \exp\left[-(|V_L| - |V_P|)\left(\frac{L - x}{\epsilon}\right) \right] \right\} \qquad (13)$$

For particles with $|V_P| < |V_L|$ Equation 13 predicts a concentration of C_F at $x = L$. Further down the tube, the concentration increases and approaches a limiting value given by

$$C = C_F \frac{|V_L|}{|V_L| - |V_P|} \qquad (14)$$

For particles with $|V_L| < |V_P|$ the predicted concentration at $x = L$ is again C_F. The concentration then increases exponentially as x decreases.

A rigorous solution to the transient case presented considerable difficulty. Later on, an approximate transient solution will be presented.

In the foregoing equations liquid velocity and diffusivity are based on that portion of the reactor cross section which is occupied by liquid rather than on the superficial cross section. Equations 15 and 16 give the relationship between the "actual" and superficial quantities:

$$V_L = \frac{V_{Ls}}{1 - \phi} \qquad (15)$$

$$\epsilon = \frac{\epsilon_s}{1 - \phi} \qquad (16)$$

Experimental Work

Apparatus. A diagram of apparatus is given in Figure 1. Experiments were conducted in a glass tube 1.8 inches in i.d. and 4 feet long. Sampling taps were mounted on the side of the tube, spaced 6 to 10 inches apart. Clear liquid and concentrated catalyst slurry were mixed in a continuous-flow stirred flask to provide the desired slurry feed to the tube. The concentrated catalyst slurry was metered through a Sigma pump. The clear liquid flow rate was determined by

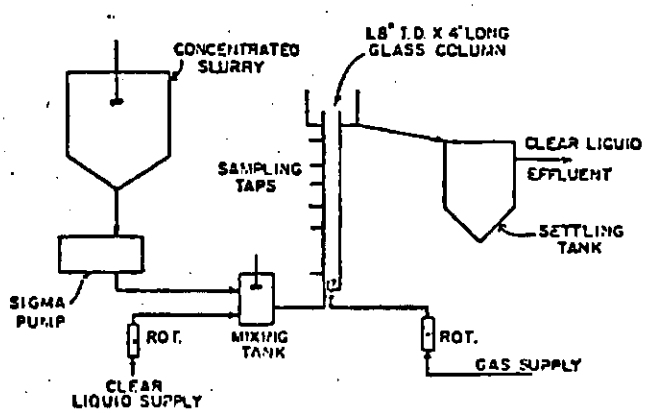

Figure 1. Schematic diagram of concurrent flow apparatus

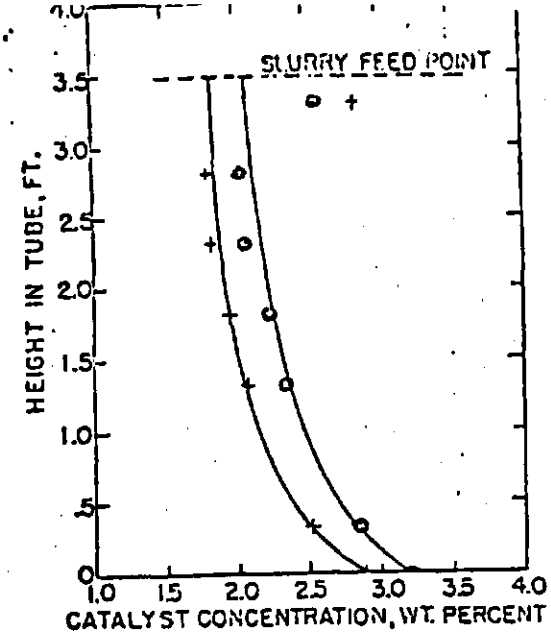

Figure 2. Concentration profile for Raney nickel catalyst in acetone in countercurrent tube

+ Experimental data for V_{LS} = 7.4 ft./min., V_{GS} = 1.1 ft./min., C_F = 2.9%
o Experimental data for V_{LS} = 12.4 ft./min., V_{GS} = 1.1 ft./min., C_F = 3.2%
— Calculated profiles for above conditions

rotameter. The gas entered the tube at the bottom through a sintered stainless steel gas disperser, which for the water experiments was in the form of a hollow cylinder; for acetone, in the form of a horizontal disk. The effluent was passed through a large settling tank for recovery of the catalyst particles. Clear liquid from the settling tank was either sewered (water experiments) or recycled to the tube (acetone experiments).

Experimental Procedure. In commencing a run, the gas feed to the tube was started first and set at the desired magnitude. The slurry feed was then started. For the concurrent flow case all flow rates were then held constant for the desired length of the experiment. During this time samples of the effluent from the tube were obtained. At the end of this time samples were taken from the sampling taps, beginning at the top of the tube and working down. Care was taken to flush the taps clear of settled solids and to remove the samples at a flow rate sufficient to prevent settling of solids in the lines. In the case of countercurrent flow (where steady state could be achieved in a reasonable length of time) the flows of slurry and gas were maintained constant until steady state had been reached. Arrival at this point was indicated by equality of the catalyst concentrations in the liquid feed and effluent streams. Samples from the tube were then taken starting at the bottom and working up.

Samples were analyzed by two methods. In the case of water, density measurements with a pycnometer gave the concentration of catalyst in the sample. In the case of acetone, the catalyst was sucked dry on a tared sintered glass funnel under an inert atmosphere. Weighing of the dried catalyst then allowed calculation of the catalyst concentration in the sample. The variables and range of variables studied were:

For Water	
Superficial liquid velocity, ft./min.	0.9–4.5
Superficial gas velocity, ft./min. (STP)	3.6–15.0
Run time, hours	2–8
For Acetone	
Superficial liquid velocity, ft./min.	0.6–3.0
Superficial gas velocity, ft./min.	3.6–15.0
Run time, hours	2–8

the experiments was determined by the sedimentation technique, because it measures particle fall velocities directly. Since fall velocity enters into the calculation of concentration profiles, a sedimentation method is ideal for these measurements.

An Andreason sedimentation pipet was used. Dilute slurry was placed in the sedimentation vessel and allowed to equilibrate in a constant temperature bath. The pipet was shaken to disperse the slurry and then replaced in the bath. Starting at this time, samples were withdrawn at selected times from a point 20 cm. below the liquid surface. Fall velocity distribution was then calculated according to the following reasoning: At a given time, t, all particles remaining in the slurry at the sampling point had fall velocities equal to or less than $20/t$ cm. per unit time. From measurements of concentration in a series of such samples, a plot of fall velocity distribution was developed. Stokes' law was used to translate fall velocity into particle diameter:

$$d_p = \sqrt{\frac{18\,\mu V_f}{g\Delta\rho}} \qquad (17)$$

Since these particle distributions followed the log-normal distribution law, they were plotted as d_p on a logarithmic scale against weight fraction on a probability scale.

Sedimentation experiments were carried out with Raney nickel catalyst in water and a number of organic liquids. From these measurements the log-normal distribution function parameters were calculated, $\bar{d}$ = 15.7 microns median particle diameter and σ_L = 2.06. Fall velocities for acetone and for the reaction masses in the countercurrent reactors were calculated using these parameters.

Discussion of Results

Particle Mixing. One problem in the calculation of catalyst profiles is the need for an appropriate diffusivity for the solid particles. In the following applications it has been assumed that the diffusivity for the solids is the same as for the liquid. The validity of the assumption is demonstrated by the work of Kalinske and Pien (3) on the suspension of sand in flowing streams. Further verification was given by experiments in which gas was blown through water containing particles of sand in the 1.8-inch tube. The diffusivity for the

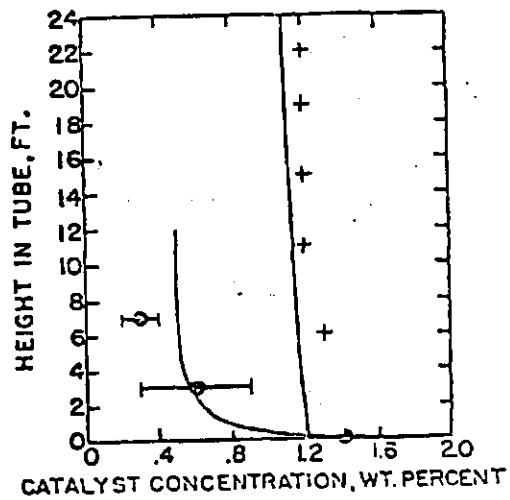

Figure 3. Concentration profile for Raney nickel catalyst in countercurrent hydrogenation plant and pilot plant units

+ Experimental data for plant unit 17.6 inches in diameter by 24 feet long
)–o–(Range of experimental data for pilot plant unit 3.5 inches in diameter by 9 feet long
——— Calculated profiles for above conditions

and particles was essentially the same as that measured for pure water (1) under the same conditions of flow rate. There are, of course, regions in which this assumption will be invalid—for example, large heavy particles in a highly fluid medium would obviously be little affected by normal mixing motions of the liquid. Peskin (2) and Friedlander (3) discuss this subject at length.

Liquid diffusivities used in the calculations below were taken from or estimated from the work of Argo and Cova (1).

Countercurrent Case. Two countercurrent catalyst suspension experiments in acetone were carried out. Catalyst profiles were calculated using Equation 10 in conjunction with a log-normal distribution function for particle size. The total catalyst concentration at any level was then calculated by the following equations:

$$C = \int_0^{d_{p\infty}} \left(\frac{\exp\left\{ \frac{-\left[\ln (d_p) - \ln \overline{d_p}\right]^2}{2 (\ln \sigma_L)^2} \right\}}{\sqrt{2\pi} \times \ln \sigma_L} \right) \times C_P \left\{ \frac{|V_L|}{|V_L| + |V_T|} + \left(1 - \frac{|V_L|}{|V_L| + |V_T|}\right) \exp\left[\frac{-(|V_L| + |V_T|)x}{\epsilon} \right] \right\} d[\ln (d_p)] \quad (18)$$

and Stokes' law,

$$V_T = \frac{g \Delta\rho (d_p)^2}{18 \mu} \quad (19)$$

Where the particle Reynolds number was greater than 1.0, Stokes' law was replaced by the more general equation:

$$V_T = \sqrt{\frac{4}{3} \frac{g d_p \Delta\rho}{\rho_L C^*}} \quad (20)$$

where C^* is the drag coefficient and is a function of particle Reynolds number.

From Figure 2 it can be seen that correlation between theory and experiment is excellent except near the top of the tube, where deviation is caused by a rapid increase in the experimental concentration. Equation 10 does not predict this sudden increase, which is caused by the configuration of the slurry feed inlet. Very likely this could be taken into account in the theoretical development by assuming that the catalyst particles enter the tube with zero fall velocity. Since a short finite (though calculable) time is required for the particles to accelerate to terminal fall velocities, there would be a narrow band at the top of the tube where particle concentration would be greater than at lower levels in the tube. Because of mixing, however, this band is spread out, giving a region of high catalyst concentration, as is seen in Figure 2. Consideration of this in the theory would involve replacing a constant fall velocity by one which is a function of residence time of the particles and then solving Equation 5 for the transient state in order to obtain particle residence time distributions.

Experimentation on a plant-scale hydrogenation unit afforded an opportunity for further checking the validity of the model and its application to larger and operating gas-feed tubular reactors. Experimental data were obtained on the plant unit (1½-foot diameter by 24-foot length) and on the pilot unit (2.5 inch-diameter by 9-foot length). Catalyst profiles for these two reactors were calculated and Figure 3 shows that again good correlation was obtained.

Figure 3 indicates the large differences in characteristics between laboratory and plant scale reactors of this type. These differences arise in terms of the respect to mixing. Thus, in the plant reactor, a high level of mixing gives rise to highly uniform catalyst concentrations throughout the volume of the reactor. In the pilot plant reactor with a much lower level of mixing, catalyst concentrations were generally lower and varied considerably with height in the reactor.

Concurrent Case. The difficulty in finding a rigorous solution of the concurrent case led to an attempt to find an approximate solution. Consider the catalyst as divided into various fractions according to size. To each fraction an average fall velocity may be assigned by means of Stokes' law. Fractions with small and intermediate fall velocities will achieve steady-state concentrations in the tube. For these fractions the catalyst profile is calculated by Equation 13 for the steady state. Fractions with large fall velocities will not achieve steady state because they tend to build up to high concentrations in the tube. For these fractions the assumption is made that the concentration at any time at any level in the tube is some fraction of the steady-state concentration at that level and that this fraction varies only with time (not with level in the tube). With this assumption it is then relatively easy to calculate transient state catalyst concentration. Intuitively, this assumption is reasonable.

It is now necessary to consider some further mathematical development. With the above stated assumption, the time-dependent and position-dependent portions of the concentration function are readily separable. Thus, this function may be written as

$$C(x,t) = G(t) \times C_s(x) \quad (21)$$

where $G(t)$ is the above-mentioned fraction (a function of time only) and $C_s(x)$ represents the steady-state concentration at point x (a function of x only).

The form of $G(t)$ can be determined by a material balance on the particles over the entire tube for the time interval t between t and $t + dt$. This yields the following equation:

$$L \frac{d[\overline{C_{av}}(t)]}{dt} = V_L C_P - V_L C_o(t) \quad (22)$$

where $C_{av}(t)$ = average concentration in the tube at time t (a function only of t), and $C_o(t)$ = concentration of particles in the effluent stream at time t (a function only of t).

Now,

$$L C_{av}(t) = \int_0^L C(x,t)dx = G(t) \times \int_0^L C_s(x)dx \quad (23)$$

and

$$C_o(t) = G(t) \times C_s(L) = G(t) C_P \quad (24)$$

Substituting into Equation 22 and integrating there is obtained:

$$\ln [1 - G(t)] = \frac{V_L \times C_P \times t}{\int_0^L C_s(x)dx} + A \quad (25)$$

One boundary condition is required.

$$\text{At } t = 0,\ G(t) = 0 \quad (26)$$

The final equation is then:

$$G(t) = 1 - \exp\left(\frac{-V_L \times C_P \times t}{\int_0^L C_s(x)dx} \right) \quad (27)$$

The quantity $\int_0^L C_s(x)\,dx$, is readily evaluated by integration of Equation 13:

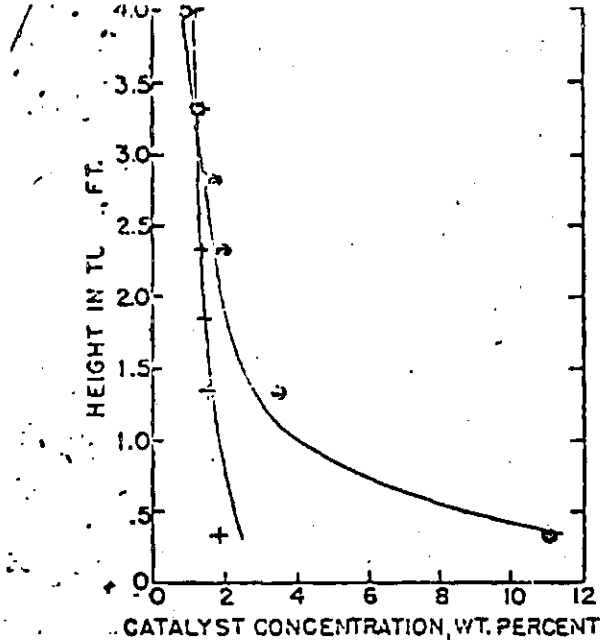

Figure 4. Effect of liquid velocity on distribution of Raney nickel catalyst in water in concurrent tube

- ● Experimental data for V_{GS} = 3.4 ft./min., V_{LS} = 1.0 ft./min., C_F = 0.9%, run time = 2.7 hours
- \+ Experimental data for V_{GS} = 3.4 ft./min., V_{LS} = 2.7 ft./min., C_F = 1.3%, run time = 1.3 hours
- — Calculated concentration profiles for above conditions

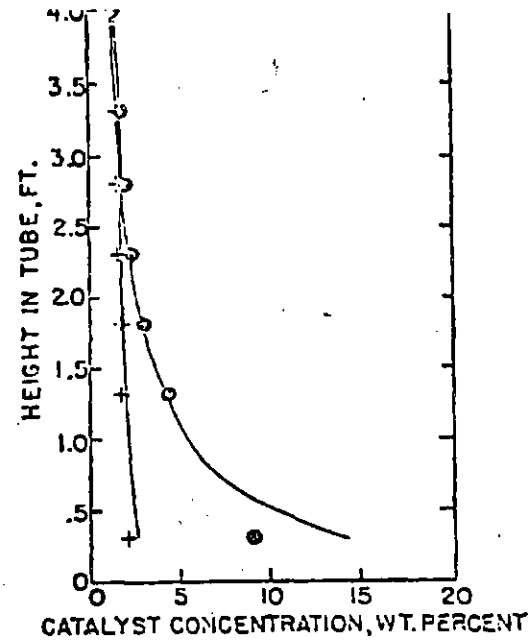

Figure 6. Effect of liquid viscosity on distribution of Raney nickel catalyst in concurrent tube

- ● Experimental data for acetone, V_{LS} = 1.3 ft./min., V_{GS} = 13.6 ft./min., C_F = 1.2%, run time = 7.6 hours, μ = 0.33 cp.
- \+ Experimental data for water, V_{LS} = 2.7 ft./min., V_{GS} = 3.4 ft./min., C_F = 1.3%, run time = 1.3 hours, μ = 0.90 cp.
- — Calculated concentration profiles for above conditions

$$\int_0^L C_L(x)dx = C_F\left(\frac{|V_L| \times L}{|V_L| - |V_F|} + \frac{\epsilon}{|V_L| - |V_F|}\left(1 - \frac{|V_L|}{|V_L| - |V_F|}\right)\left\{1 - \exp\left[-(|V_L| - |V_F|)\frac{L}{\epsilon}\right]\right\}\right) \quad (28)$$

Now, by use of Equations 13, 21, 27, and 28 it is possible to calculate $C(x,t) = G(t) \times C_L(x)$. This gives the concentration profile for catalyst of a given fall velocity. By splitting up a catalyst into a large number of fractions according to size and calculating an average fall velocity for each fraction, the concentration profile can be calculated by the above equations for each fraction of catalyst. By summing up these concentrations, the total concentration profile for the catalyst is obtained.

Typical results of these calculations are shown in Figures 4, 5, and 6, where a comparison may be drawn with experimental data. As can be seen, the calculated curves are consistent with the experimental data. Good correlation is obtained everywhere except in one case, where large catalyst concentrations are encountered. This discrepancy may be explained by slower settling of particles in concentrated slurries (hindered settling) and the build-up of particles on the reactor floor below the gas sparger. Both effects would cause lower experimental concentrations.

Figures 4, 5, and 6 show the effects of liquid velocity, gas velocity (through its effect on liquid mixing), and liquid viscosity (through its effect on V_F), respectively. Thus, higher gas and liquid velocities and higher viscosities all tend to give more uniform catalyst distributions.

In summary, it may be stated that the mathematical model applied here gives results consistent with experimental observations. Such calculations should be of value in tubular reactor design and scale-up where slurry-type catalysts are involved.

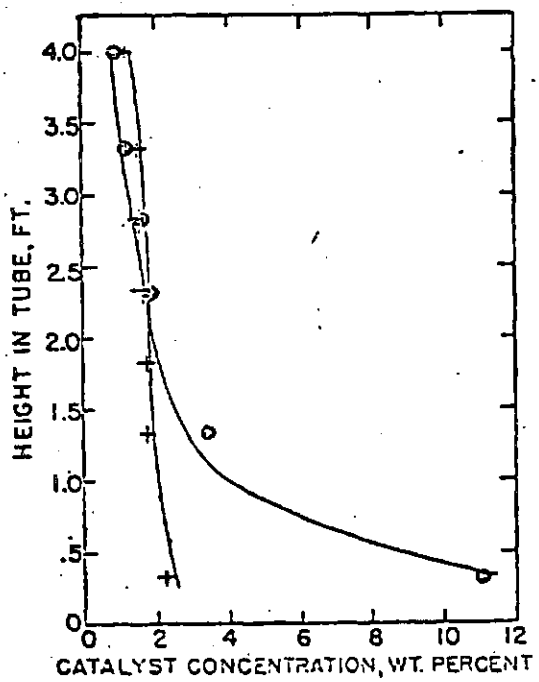

Figure 5. Effect of gas velocity on distribution of Raney nickel catalyst in water in concurrent tube

- ● Experimental data for V_{GS} = 3.4 ft./min., V_{LS} = 1.0 ft./min., C_F = 0.9%, run time = 2.7 hours
- \+ Experimental data for V_{GS} = 14.2 ft./min., V_{LS} = 1.0 ft./min., C_F = 1.1%, run time = 3.2 hours
- — Calculated concentration profiles for above conditions

= variable of integration
= concentration of catalyst, lb. catalyst/cu. ft. slurry
= average concentration in tube
= concentration of catalyst in feed stream
= concentration of catalyst at point l in reactor
= concentration of catalyst in effluent stream at time t
= concentration of catalyst at point x at steady state
= drag coefficient
= particle diameter, microns
= diameter of largest particle in integration over particle size distribution, microns
= exponential function
= acceleration of gravity, ft./sec.^{2}
= time-dependent portion of concentration function, dimensionless
= length of reactor, ft.
= natural logarithm
= median particle diameter, microns
= mass flux of liquid in longitudinal direction, lb./sq. ft. sec.
= mass flux of particles, a vectorial quantity, lb./sq. ft. sec.
= mass flux of particles in longitudinal direction, lb./sq. ft. sec.
= time, sec.
= fall velocity of particle through still liquid, ft./sec.
= superficial gas velocity, ft./min.
= liquid velocity, ft./sec.
= superficial liquid velocity, ft./min.
= particle velocity with respect to laboratory coordinates, ft./sec.
$|\ |$ = absolute value of quantity between brackets
ϵ = eddy diffusivity in liquid, sq. ft./sec.
ϵ_s = superficial eddy diffusivity, sq. ft./sec.
ρ = density of slurry, lb./cu. ft.
ρ_L = density of liquid, lb./cu. ft.
$\Delta\rho$ = difference between particle and liquid densities, lb./cu. ft.
μ = liquid viscosity, cp.
σ_L = particle diameter at which 15.87% of particles have a greater diameter divided by median particle diameter
ϕ = gas fraction; fraction of reactor volume occupied by gas

References

(1) Argo, W. B., Cova, D. R., IND. ENG. CHEM. PROCESS DESIGN DEVELOP. 4, 352 (1965).
(2) Friedlander, S. K., *A.I.Ch.E. J.* 3, 381–5 (1957).
(3) Kalinske, A. A., Pien, C. L., "Experiments on Eddy-Diffusion and Suspended-Material Transportation in Open Channels," Transactions of American Geophysical Union, 24th Annual Meeting, Section of Hydrology, pp. 530–5, 1943.
(4) O'Brien, M. O., *Trans. Am. Geophys. Union* 14, 487–91 (1933).
(5) Peskin, R. L., "Diffusivity of Small Suspended Particles in Turbulent Fluids," A.I.Ch.E. National Meeting, May 20–23, 1962
(6) Siemes, W., Weiss, W., *Chem. Ing. Tech.* 29, 727–32 (1957).
(7) van de Vusse, J. G., *Chem. Eng. Sci.* 10, 229–33 (1959).

RECEIVED for review February 18, 1965
ACCEPTED August 13, 1965

1,6 gas influence on mixing

MULTICOMPONENT FIXED-BED SORPTION OF INTERFERING SOLUTES

System Behavior under Asymptotic Conditions

DAVID O. COONEY AND EDWIN N. LIGHTFOOT

Department of Chemical Engineering, University of Wisconsin, Madison, Wis.

The equations which describe asymptotic concentration profiles in single-solute fixed-bed separations and exchange processes are extended to multicomponent systems. The elution, with water, of an ion exchange resin bed uniformly presaturated with an aqueous sodium chloride–glycerol solution is discussed as an illustrative example. Experimental data for the process agreed well with prediction.

A SOLUTE concentration profile generated in a fixed-bed saturation or elution operation tends to develop with time in one of two basic ways. Depending on the general nature of the distribution relationship, the solute "front" will be either continuously broadening or self-sharpening in nature. In the former case, the asymptotic limit of the profile consists of an infinitely broad front, while in the latter situation the asymptotic state is a relatively sharp S-shaped front of invariant form—that is, a "constant-pattern" front. Only solute fronts having this (nontrivial) asymptotic shape are considered in this paper.

The complete description of the shape of the moving-phase solute concentration profiles for any solute as a function of time may, in either case, be obtained by solving simultaneously the equation of continuity and a mass transfer rate expression for the solute, under appropriate boundary conditions. Even for single-solute systems, however, analytical solutions to these equations are generally attainable only for cases of zero longitudinal dispersion and linear equilibria, or for a few special types of nonlinear equilibria. Thus, in many instances, one must either perform a two-dimensional numerical integration of the continuity and rate equations or use a lengthy approximate procedure (*19, 20*).

If, however, one is primarily interested in the determination of effluent curves alone (as is normally the case in column design work) and if the process involves the travel of a self-sharpening front over a reasonable distance, a simple approximate description of the system, adequate for most design purposes, may usually be attained by assuming that the system reaches its asymptotic state within the bed. This assumption offers a considerable advantage, for it permits the reduction of the system continuity equations from partial to ordinary differential equations. While this may still not lead to an analytical solution, it vastly decreases amount of numerical calculation time required for solution.

In practice, we can expect the assumption of constant-